Effects of irrigation on global climate during the 20th century

M. J. Puma[1,2] and B. I. Cook[2,3]

Received 1 March 2010; revised 7 May 2010; accepted 21 May 2010; published 28 August 2010.

[1] Various studies have documented the effects of modern-day irrigation on regional and global climate, but none, to date, have considered the time-varying impact of steadily increasing irrigation rates on climate during the 20th century. We investigate the impacts of observed irrigation changes over this century with two ensemble simulations using an atmosphere general circulation model. Both ensembles are forced with transient climate forcings and observed sea surface temperatures from 1902 to 2000; one ensemble includes irrigation specified by a time-varying data set of irrigation water withdrawals. Early in the century, irrigation is primarily localized over southern and eastern Asia, leading to significant cooling in boreal summer (June–August) over these regions. This cooling spreads and intensifies by century's end, following the rapid expansion of irrigation over North America, Europe, and Asia. Irrigation also leads to boreal winter (December–February) warming over parts of North America and Asia in the latter part of the century, due to enhanced downward longwave fluxes from increased near-surface humidity. Precipitation increases occur primarily downwind of the major irrigation areas, although precipitation in parts of India decreases due to a weaker summer monsoon. Irrigation begins to significantly reduce temperatures and temperature trends during boreal summer over the Northern Hemisphere midlatitudes and tropics beginning around 1950; significant increases in precipitation occur in these same latitude bands. These trends reveal the varying importance of irrigation-climate interactions and suggest that future climate studies should account for irrigation, especially in regions with unsustainable irrigation resources.

Citation: Puma, M. J., and B. I. Cook (2010), Effects of irrigation on global climate during the 20th century, *J. Geophys. Res.*, *115*, D16120, doi:10.1029/2010JD014122.

1. Introduction

[2] For many regions, the rapid expansion of irrigation during the 20th century has significantly altered the hydrologic cycle and energy budget at the land surface [e.g., *Wisser et al.*, 2010], motivating research into the potential impacts that modern irrigation rates have on regional and global climate [*Boucher et al.*, 2004; *Lobell et al.*, 2006; *Sacks et al.*, 2009; *Lobell et al.*, 2009]. These studies, and others, support the notion that current irrigation significantly alters climate in some areas [*Sacks et al.*, 2009; *Lobell et al.*, 2009], with the magnitude of the climate response depending on the spatial extent of irrigation and the degree to which a region's climate regime is linked to its land surface processes [e.g., *Lobell et al.*, 2009; *Koster et al.*, 2004, 2009].

[3] One of the important direct climatic effects of irrigation is the reduction of surface air temperature through shifts in the Bowen ratio from sensible to latent heating [e.g., *Kueppers et al.*, 2007; *Sacks et al.*, 2009]. When irrigation-related increases in soil moisture lead to greater evapotranspiration, increased atmospheric water vapor may also enhance cloud cover, convection, and downstream precipitation [*Pielke*, 2001; *Sacks et al.*, 2009]. Irrigation effects on climate may also be indirect, especially in monsoon regions where alteration of the thermal contrast between land and ocean may produce changes in monsoon circulation and the accompanying climatic variables [e.g., *Lee et al.*, 2009; *Saeed et al.*, 2009; *Douglas et al.*, 2009]. These direct and indirect climatic responses have been widely demonstrated in numerous modeling [e.g., *Lobell et al.*, 2006; *Haddeland et al.*, 2006; *Kueppers et al.*, 2007, 2008; *Sacks et al.*, 2009; *Lobell et al.*, 2009; *Diffenbaugh*, 2009; *Saeed et al.*, 2009; *Douglas et al.*, 2009] and observational [e.g., *Barnston and Schickedanz*, 1984; *Bonfils and Lobell*, 2007; *Lee et al.*, 2009] studies. In fact, the magnitude of temperature reduction in certain regions may be comparable to or even exceed the effects of other climate forcings [e.g., *Bonfils and Lobell*, 2007; *Kueppers et al.*, 2007; *Lobell et al.*, 2009], leading to the hypothesis that the global warming signal has been "masked" in certain regions by irrigation-related cooling [e.g., *Kueppers et al.*, 2007; *Lobell et al.*, 2008; *Diffenbaugh*, 2009].

[1]Center for Climate Systems Research, Columbia University, New York, New York, USA.
[2]NASA Goddard Institute for Space Studies, New York, New York, USA.
[3]Lamont-Doherty Earth Observatory, Earth Institute at Columbia University, Palisades, New York, USA.

0148-0227/10/2010JD014122

[4] Irrigation has expanded over the course of the 20th century, even more rapidly since the 1950s and 1960s [*Freydank and Siebert*, 2008]. In 1901 the global area equipped for irrigation was approximately 53 million hectares (Mha), increasing to 285 Mha by 2002 [e.g., *Wisser et al.*, 2010]. While current irrigation may cause significant climatic changes at the regional scale, it is not known when and where these effects became significant during the 20th century. It also remains unclear how important irrigation has been relative to other changes in land use that affected a similar land area (e.g., urbanization) during the last century [*Bonfils and Lobell*, 2007]. In fact, *Sacks et al.* [2009] contend that greater attention should be given to land management dynamics such as irrigation, because they can be as important as land cover dynamics for understanding and modeling both past and future climate. Furthermore, 20th century trends in irrigation-climate interactions are relevant for efforts that estimate water resource availability and its dependence on socioeconomic conditions [e.g., *Vörösmarty et al.*, 2000; *Alcamo et al.*, 2007; *Shen et al.*, 2008]. These interactions, and their past trends, may provide valuable information on the spatiotemporal relevance of irrigation-climate feedbacks for water availability.

[5] An important open question is to understand what the transient response of 20th century climate is to the rapid increase in irrigation. Understanding how irrigation amount, extent, and location have affected climate over this century can provide insight into how future irrigation will interact with climate and the magnitude of this interaction. This transient response is also important, because irrigation effects on climate could help to explain some of the mismatches between observed and simulated climate trends over land [*Lobell et al.*, 2008]. In this study, we estimate the effects of the expansion of irrigation on 20th century climate. We follow the recent approach of *Sacks et al.* [2009], in that we attempt to apply irrigation realistically in space and time to a sophisticated land surface model, allowing the model to compute explicitly the water and energy dynamics of the land surface. This irrigation data is drawn from a new reconstruction of global hydrography for the 20th century by *Wisser et al.* [2010], who combined time-varying data sets of irrigated areas with a fully coupled water balance and transport model to estimate monthly irrigation rates over the century. We use this data set in combination with a global atmosphere general circulation model to examine, for the first time, the impact of irrigation on climate over the course of the 20th century.

2. Data and Methods

2.1. Irrigation Data

[6] Estimation of irrigation rates for the 20th century are taken from a reconstruction of global hydrography by *Wisser et al.* [2010]. Full details are in the work of *Wisser et al.* [2010], but their methodology is briefly summarized here. *Wisser et al.* [2010] first used the University of Frankfurt/FAO Global Map of Irrigated Areas [*Siebert et al.*, 2005a, 2005b] to identify the areas equipped for irrigation at a spatial resolution of 5arc minutes for the turn of the 21st century (around the year 2000). The *areas equipped for irrigation* are defined as agricultural lands that have built-in irrigation structures, although the structures might not always be in use [*Freydank and Siebert*, 2008]. From this map, they created a time series of irrigated areas in each grid cell extending back to 1901 by rescaling the year 2000 values with time series of irrigated area at the country level (compiled by *Freydank and Siebert* [2008]). Prior to 1950, country level data on areas equipped for irrigation were unavailable for many locations. In these cases, *Freydank and Siebert* [2008] linearly extrapolated back to 1900. *Wisser et al.* [2010] note that, although this irrigated area data set contains significant uncertainties due to the general unavailability of data both below the country level and for the early 20th century, it does adequately reflect the large-scale dynamics of the irrigated area development over the century.

[7] Using these irrigated area data, estimates of monthly irrigation rates were obtained using a water balance and transport model (WBMplus) [e.g., *Vörösmarty et al.*, 1998; *Federer et al.*, 2003], which includes explicit representation of human activities directly affecting the water cycle (i.e., irrigation [*Wisser et al.*, 2008] and reservoir operation [*Wisser et al.*, 2010]). In their model, crop evapotranspiration was estimated as the product of reference evapotranspiration and a time-varying crop coefficient [*Allen et al.*, 1998]. Next, a soil moisture balance was computed, and irrigation water was applied to refilled the soil to its holding capacity whenever soil moisture dropped below a crop-dependent threshold. This holding capacity is defined in WBMplus as the product of a characteristic field capacity (soil moisture at 30 kPa water potential) and a vegetation-dependent rooting depth [*Vörösmarty et al.*, 1989]. For rice paddies, *Wisser et al.* [2010] assume that a 50 mm layer of water must be maintained during the growing season and that water percolates at a constant, soil texture–dependent rate. Finally, *Wisser et al.* [2010] adjusted these irrigation amounts to compute the *gross irrigation water requirements*, which is the amount of water that actually has to be extracted from external sources (lakes, rivers, and groundwater). That is, they account for water lost during distribution and field scale application with an irrigation efficiency factor, which approximates the fraction of water used by crops relative to the amount withdrawn from irrigation sources.

[8] We spatially averaged the monthly estimates of gross irrigation water requirements from *Wisser et al.* [2010] to the resolution (2° latitude by 2.5° longitude) of the general circulation model (ModelE) described below. Although these rates could have been computed within the general circulation model, the data provide a better estimate of the actual amounts of irrigation, which are independent of the ModelE's biases. Of course, irrigation estimates from the WBMplus have uncertainties as well. For example, the WBMplus derives its daily precipitation and temperature data from monthly mean values for the period 1901 to 2002 in the CRU TS 2.1 data set [*Mitchell and Jones*, 2005], which has well-documented deficiencies [e.g., *Tian et al.*, 2007; *Adam et al.*, 2006]. In time, we assign the monthly values from *Wisser et al.* [2010] to the middle of each month and linearly interpolate to the daily level. We note that the gross irrigation estimates are used rather than the estimates of the irrigation water used by the crops (i.e., net irrigation), so that the runoff, infiltration, and water uptake physics of the ModelE can determine how much irrigation water is transpired by the vegetation.

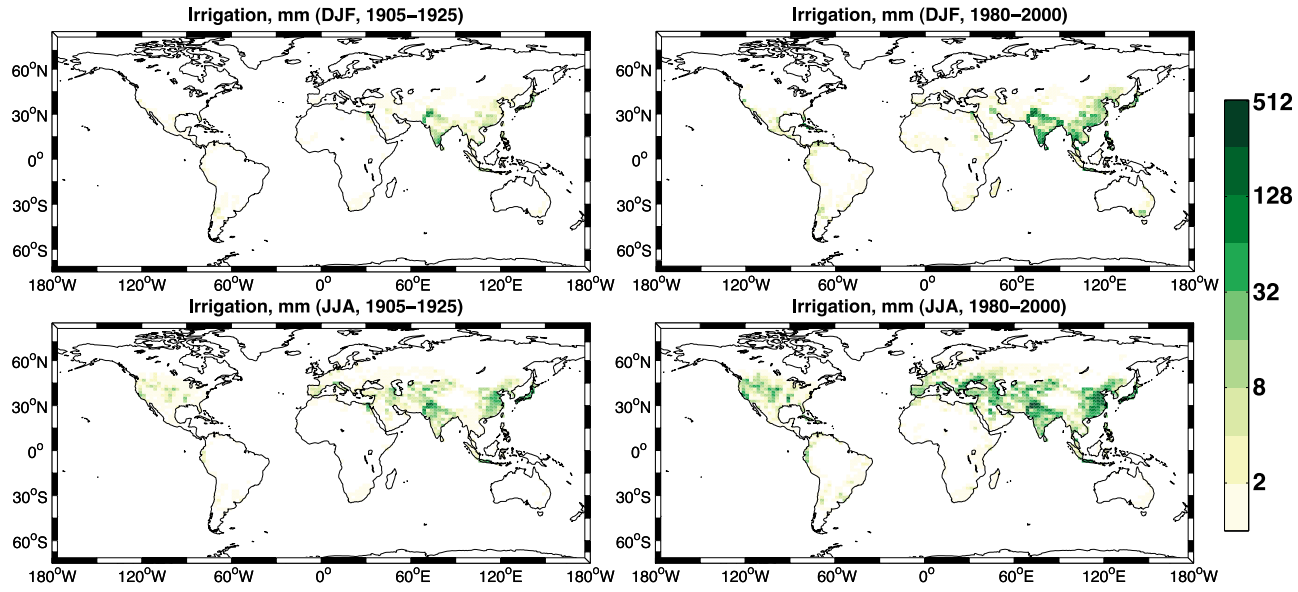

Figure 1. Global distribution of gross irrigation (mm/season) for DJF and JJA. (left) Mean for early 20th century (1905–1925). (right) Mean for late 20th century (1980–2000).

[9] The global distributions of gross irrigation during the boreal winter (December, January, and February: DJF) and summer (June, July, and August: JJA) are shown in Figure 1, averaged over the early (1905–1925) and late (1980–2000) 20th century. For the early part of the century, the largest amounts of irrigation are in Asia (especially Southern, Central, and Eastern Asia), with secondary peaks in irrigation over central North America, Southern Europe, and Western and Southeastern Asia. By the end of the century, irrigation increases in these areas and becomes more extensive, especially in Northern Europe, Central Asia, and Western Asia. For both of these periods, irrigation is greatest in the Northern Hemisphere during boreal summer (JJA).

[10] Figure 2 shows a time series of seasonal gross irrigation for five latitude bands. Gross irrigation steadily increases over the course of the 20th century (Figure 2). Highest water withdrawals for irrigation occur in the Northern Hemisphere's low latitudes (0°–30°N) and midlatitudes (30°–60°N). In these bands, irrigation withdrawals steadily increase, accelerating after about 1950. In the midlatitudes, irrigation occurs primarily during the boreal summer, when temperatures are amenable to growing crops. In the low latitudes, the primary limitation to crop growth during the dry season (DJF) is moisture, and the seasonal distribution of irrigation withdrawals is biased toward this season. These patterns are largely mirrored (if of reduced magnitude) in the southern hemisphere's low latitudes (30°S–0°) and midlatitudes (60°S–30°S). In the boreal high latitudes (60°N), irrigation amounts are quite low, which likely reflect trace amounts of irrigation in Scandinavia. Below 60°S, there is little irrigation or even arable land area, and we have omitted this graph for the sake of brevity.

2.2. Model and Simulations

[11] We use the Goddard Institute for Space Studies (GISS) ModelE to estimate irrigation effects on climate throughout the 20th century. The GISS ModelE is a state-of-the-art atmospheric general circulation model [*Schmidt et al.*, 2006], which is run at 2° latitude by 2.5° longitude horizontal resolution and with 40 vertical layers for these experiments. All of our simulations are forced with observed sea surface temperatures (SSTs) from the Hadley

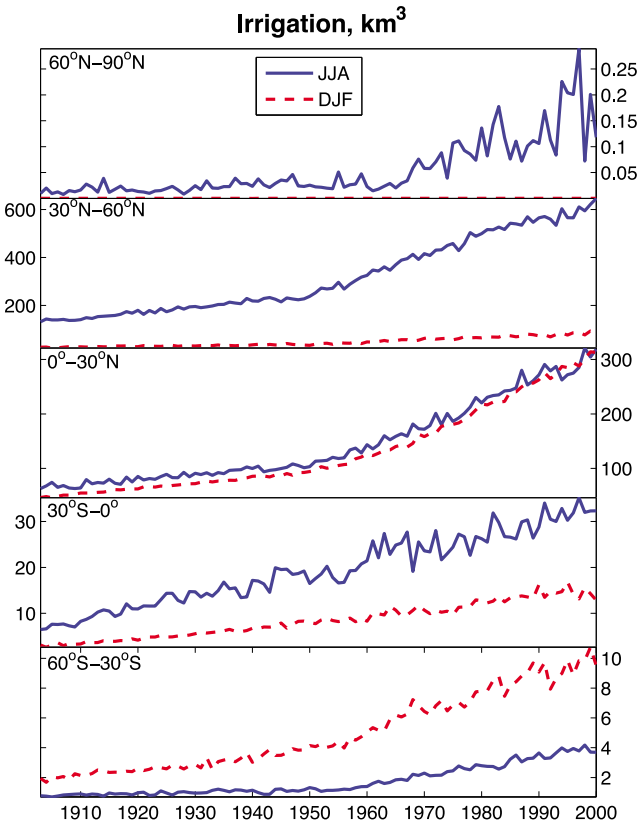

Figure 2. Seasonal gross irrigation (km^3/season) by latitude band (60°N–90°N, 30°N–60°N, 0°–30°N, 30°S–0°, 60°S–30°S) over the 20th century. Note each latitude band plot has a different scale.

Center analysis [*Rayner et al.*, 2003]. The GISS ModelE's simulation of modern-day climate compares favorably with observations, although with some notable biases, especially in the subtropical marine stratocumulus regions. *Hansen et al.* [2007] found that the GISS ModelE replicates the climate of the 20th century, including trends and low- and high-frequency variability, when forced with modern forcings and observed SSTs. Readers are referred to the available literature [*Hansen et al.*, 2007; *Schmidt et al.*, 2006] for more detailed discussions of GISS ModelE formulations and performance.

[12] The details of the current land model are primarily as described by *Schmidt et al.* [2006] and *Rosenzweig and Abramopoulos* [1997], except for updates to the model's biophysics and lake dynamics. For most grid cells, the land area is divided into two parts, corresponding to bare and vegetated soil. The soil column for each part has six layers, extending to a maximum depth of 3.5 m, with soil moisture and temperature computed separately for each column. The model distinguishes among 8 vegetation types for its photosynthesis and stomatal conductance computations, which have been revised to use the well-known functions of *Farquhar et al.* [1980] and *Ball et al.* [1987], respectively. The model does not simulate vegetation growth, but rather has prescribed vegetation cover. The natural vegetation cover is based on the work of *Matthews* [1983, 1984] and the crop cover is from *Ramankutty and Foley* [1999]. The crop cover is updated every ten years, while the relative proportions of the natural vegetation types remain constant in time. However, all vegetation (including crops) interact with soil moisture from the single vegetated soil column. This limitation of the GISS ModelE has implications for our irrigation methodology and predictions, which we will discuss further in subsequent sections.

[13] We modify the GISS ModelE to represent irrigation by adjusting the land and lakes routines. In the absence of irrigation, soil moisture values for the bare and vegetated columns change as a function of surface evaporation from the first layer, transpiration (only for the vegetated column), infiltration, vertical transport between soil layers, and underground runoff [*Rosenzweig and Abramopoulos*, 1997]. Irrigation is modeled through addition of an irrigation flux at the top of the vegetated column, below the vegetation canopy, at the daily rates described in the previous section. For days with nonzero irrigation, this flux is kept constant over the course of the day and is applied for every subdaily time step. The irrigation water either infiltrates the soil column or leaves the grid cell as surface runoff. This infiltrating irrigation water can then be removed from the soil column through evapotranspiration and underground runoff, such that that the model will have an irrigation efficiency that depends on the ModelE's climate and land surface properties.

[14] The realism of the hydrological processes represented in the ModelE first depends on the crop type (rice versus nonrice) within a grid cell. For nonrice crops, the modeling scheme is consistent with the main physical processes controlling hydrological dynamics. However, the land surface dynamics of rice crops are very different and are likely more similar to the physical characteristics of wetlands. Additional work is needed to understand the impact of this model shortcoming. Our scheme's realism depends also on irrigation timing, which varies depending on actual irrigation methods (e.g., flood, furrow, micro, or sprinkler irrigation) and crop type. One possible difference among these irrigation scenarios, which would lead to varying irrigation impacts on climate, is the extent to which soil-water availability limits evapotranspiration. In fact, *Lobell et al.* [2009] argued that irrigation timing is important when it affects the length of time that soil moisture is below the threshold value at which soil moisture begins to limit transpiration. For example, if a region's irrigation is biweekly and soil moisture limits evapotranspiration for a significant portion of the 2 week period, then this study's daily irrigation scheme would likely overestimate evapotranspiration. However, in terms of the subdaily distribution of irrigation, *Sacks et al.* [2009] performed offline sensitivity tests comparing the climatic effects of applying the same daily irrigation volume over 24 h, over a single hour beginning at midnight, and over a single hour beginning at noon at constant rates. The authors found relatively small differences (~1%) in latent heat fluxes and ground temperatures, although they pointed out that the responses might have been dampened by a lack of atmospheric feedbacks in their offline simulations.

[15] We attempt to conserve water and energy within the model by withdrawing irrigation water and energy from the surface water in the grid cell, which includes local lakes and rivers. However, if this surface water is insufficient to meet the irrigation demand, then the remaining required water is added to the system with the assumption that these water withdrawals are occurring from groundwater systems that are disconnected from the hydrologic cycle (i.e., fossil groundwater) [e.g., *Wisser et al.*, 2010]. This fossil water is added at the temperature of the first soil layer. Although we apply a realistic amount of irrigation water, our total irrigated area is overestimated, because we apply the irrigated water to the total vegetated fraction of a grid cell, rather than just the cropped fraction.

[16] We conducted two 5-member ensemble simulations using observed SSTs and climate forcings from 1902 to 2000, with each ensemble member starting from unique initial conditions. One ensemble is our control (CTRL) run without irrigation; the second ensemble also includes the irrigation water fluxes as described previously (IRRIG). Unless otherwise noted, discussions are focused on differences between the two simulations in the ensemble means, which are computed only for grid cells containing land. We analyze model output starting in 1905 to allow for the effects of soil moisture spin up during the first three years. All anomalies are calculated relative to a 1905–2000 baseline from the CTRL run. All difference plots are IRRIG minus CTRL and, because we are primarily interested in land surface climate, differences over the oceans are masked out.

3. Results

3.1. Climate Responses to Observed Irrigation: 1905–1925 and 1980–2000

[17] Irrigation has the greatest potential to alter climate directly when it can significantly increase evapotranspiration, reducing the ratio of sensible to latent heating (Bowen ratio) (Figure 3). In the early part of the century (1905 evapotranspiration has intensified on the Indian subcontinent. These changes are attributable to irrigation-related increases in soil moisture (Figure 1).

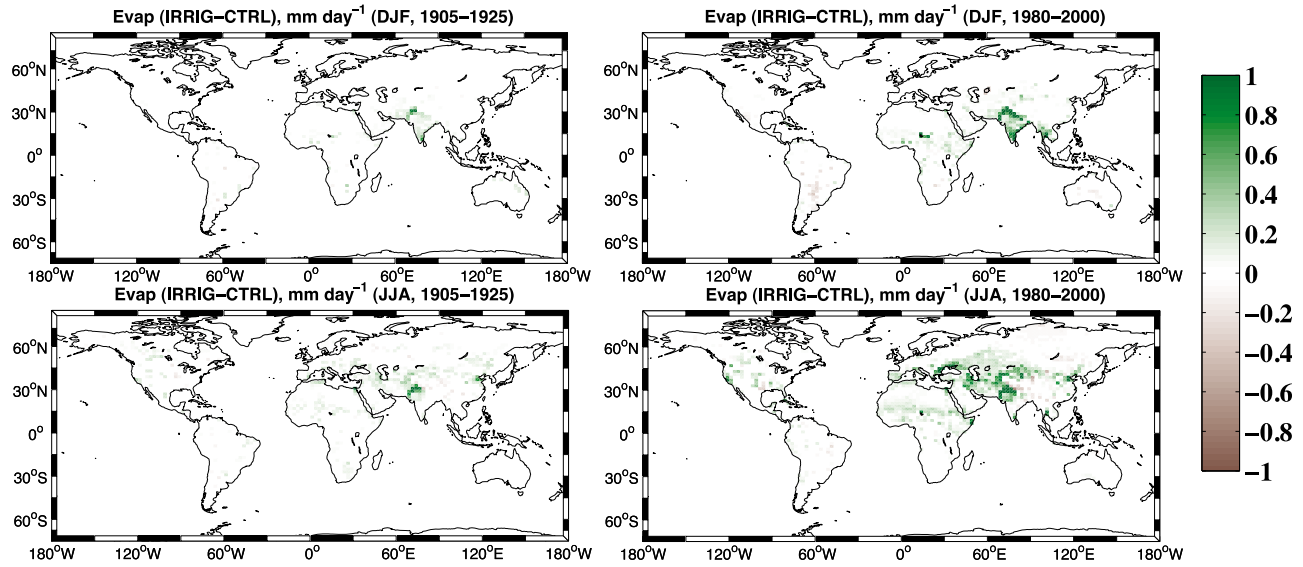

Figure 3. Change in seasonal evapotranspiration (mm d^{-1}) induced by irrigation (IRRIG minus CTRL run) for DJF and JJA. (left) Mean for early 20th century (1905–1925). (right) Mean for late 20th century (1980–2000). Only changes that are over land (60°S–90°N) and have a significance level of $p < 0.1$ (based on two sample t test) are presented.

[18] For boreal summer (July–August, JJA) in the early 20th century, the largest evapotranspiration increases are still over Southern Asia at the beginning of the century, with some minor increases in other areas that also have irrigation (Eastern Asia, Europe), coinciding with the major growing season in these regions. By century's end, increases in JJA evapotranspiration are found extensively throughout the Northern Hemisphere. Many of the areas with larger evapotranspiration overlap with the JJA irrigated areas. One notable exception is the Sahel region of West Africa; evapotranspiration increases found in the Sahel region are due to enhanced precipitation (i.e., an indirect irrigation effect), rather than the relatively low-irrigation inputs into this region.

[19] Evapotranspiration does not increase for the majority of China's heavily irrigated regions. To understand this result, we look at the ModelE's evaporative regime (not shown). For China's irrigated areas in the control run, evapotranspiration is limited by energy, whereas other irrigated areas in North America and the Indian subcontinent are typically soil moisture limited. Furthermore, irrigation in China is primarily for rice cultivation, which typically requires standing water. Therefore, even though a region is characterized by an energy-limited evaporative regime (i.e., soil moisture does not limit evapotranspiration), irrigation is still often required for rice paddies. Interestingly, we find that the few grid cells in China with the largest temperature response to irrigation (in the vicinity of Beijing) are also the grid cells with the lowest evaporative fraction. However, we note that predictions of evaporative fraction are model dependent because of differences in the land surface's representation and parameterization among climate models. Adding to this model uncertainty is the fact that the hydrological dynamics of rice paddies are poorly represented in the ModelE and other land models, because they lack realistic representation of water table dynamics.

[20] Cloud cover changes are a potential consequence of the direct evapotranspiration increases, and may impact climate through changes in incoming radiation or precipitation. In Figure 4, we see greater amounts of cloud cover for many regions, but we also find that the increases do not directly map to the most highly irrigated areas. For 1905–1925, sporadic increases in cloud cover are found during DJF throughout Asia but are absent from the Indian subcontinent. A portion of the Sahara Desert also has a sizable area of increased cloud cover. During the latter part of the century, cloud cover increases are found over the Aral Sea region, parts of Southern and Southeastern Asia, and the northern portions of sub-Saharan Africa.Decreases in cloud cover are less extensive but occur in Mexico and sporadically for the other continents. As for the boreal winter, the JJA cloud cover is also larger for portions of the Sahara Desert during the 1905–1925 period. Enhanced cloud cover is also evident in Central Europe and portions of Central and Eastern Asia. By the end of the 20th century, JJA cloud cover has increased over much of Eurasia and the Sahara. Small increases (~2%) are also found in Southern Africa and sporadically throughout the Americas. Importantly, one major area of decrease occurs in the eastern portion of the Indian subcontinent, which is related to the weakening of this region's monsoon in our IRRIG ensemble.

[21] As with evapotranspiration and cloud cover, temperature (Figure 5) and precipitation (Figure 6) responses generally scale with the magnitude of irrigation water inputs (Figure 1). Early in the century, direct irrigation-induced cooling (~1–2 K) is primarily localized over the regions with highest irrigation and highest evapotranspiration: the Indian subcontinent (DJF) and Central Asia (JJA). However, most of Eastern Asia does not cool significantly, despite high-irrigation rates in DJF and JJA (except for portions of northeast China and Korea). This result is consistent with the earlier finding that evapotranspiration is limited by

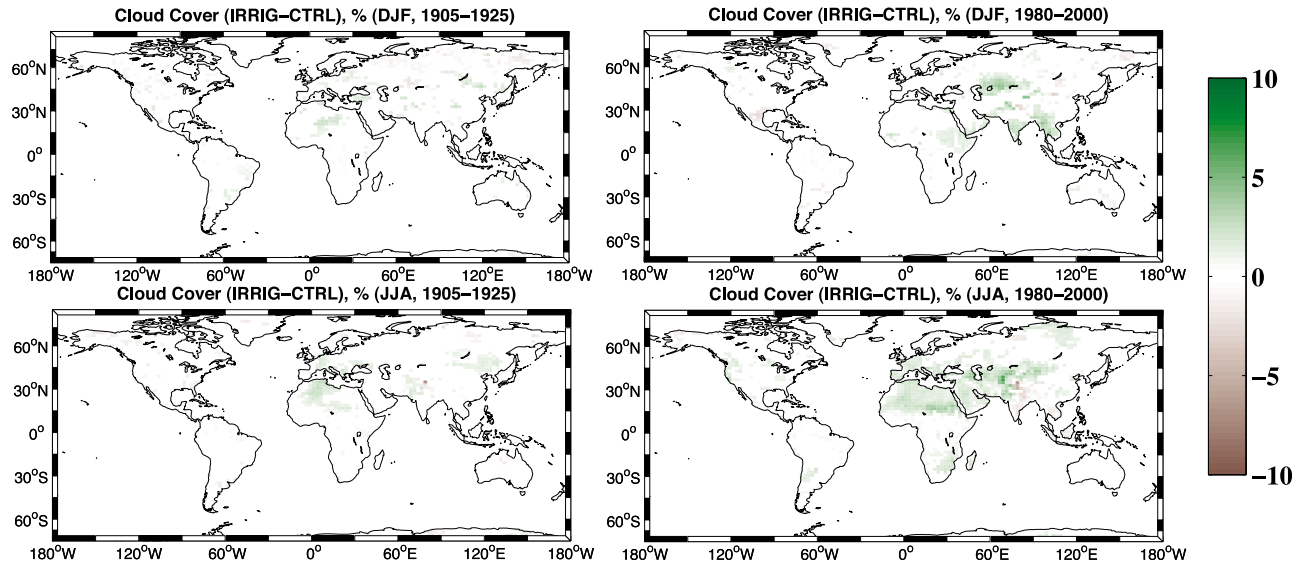

Figure 4. Change in seasonal cloud cover (%) induced by irrigation (IRRIG minus CTRL run) for DJF and JJA. (left) Mean for early 20th century (1905–1925). (right) Mean for late 20th century (1980–2000). Only changes that are over land (60°S–90°N) and have a significance level of $p < 0.1$ (based on a two sample t test) are presented.

energy rather than by soil moisture in this region. Limited cooling can also be seen in western North America and Europe. This cooling generally intensifies and expands with additional irrigation inputs by the end of the century. The largest cooling (~3 K) is still in the northwestern portions of the Indian subcontinent, but now areas of significant cooling (~0.5 K) have expanded throughout Asia, Europe, North America, and even the Sahel region of Africa. Cooling in these regions is primarily due to a shift in the Bowen ratio from sensible to latent heating that occurs with the addition of water to the soil. However, we note that the cooling of the Sahel region is not directly related to irrigation, because irrigation rates are quite low in all seasons over West Africa.

[22] Areas of significant warming (~0.5 to 2 K) are also apparent. Over eastern India, this warming is due to drier soils and enhanced sensible heat fluxes from a weakened Indian monsoon, driven by a cooler Asian land surface and reduced land-sea temperature contrast. Other large areas of warming are apparent over regions of Asia and North America during DJF. This warming comes directly from enhanced downwelling longwave radiation due to increased near surface specific humidity over these areas. The

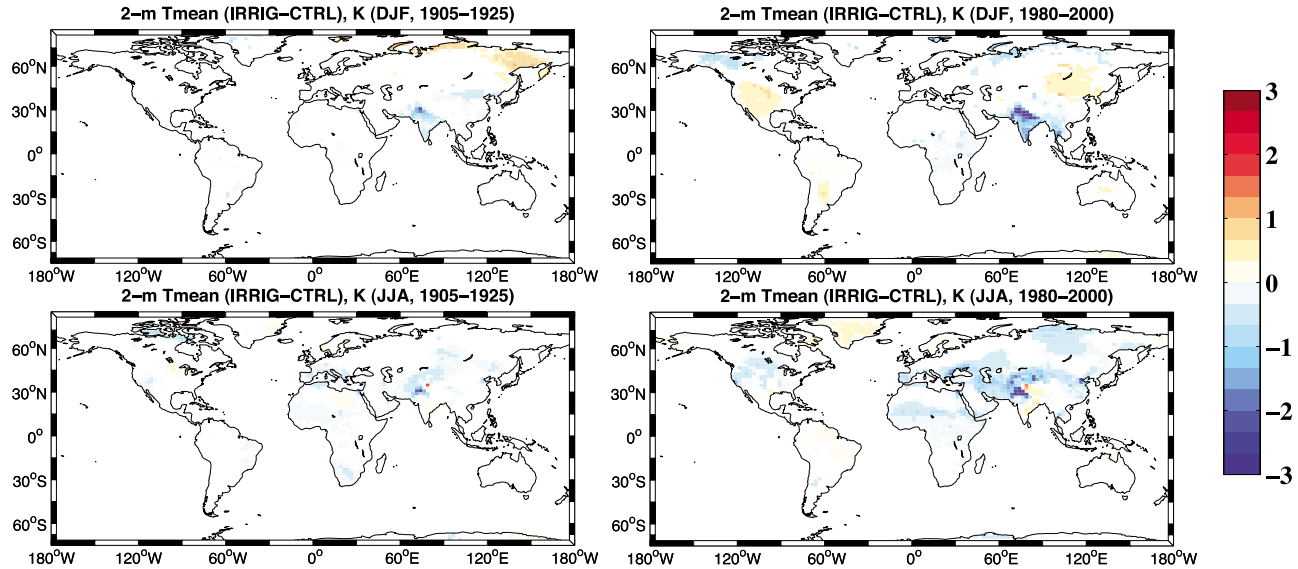

Figure 5. Change in seasonal 2 m air temperature (K) induced by irrigation (IRRIG minus CTRL run) for DJF and JJA. (left) Mean for early 20th century (1905–1925). (right) Mean for late 20th century (1980–2000). Only changes that are over land (60°S–90°N) have a significance level of $p < 0.1$ (based on a two sample t test) are presented.

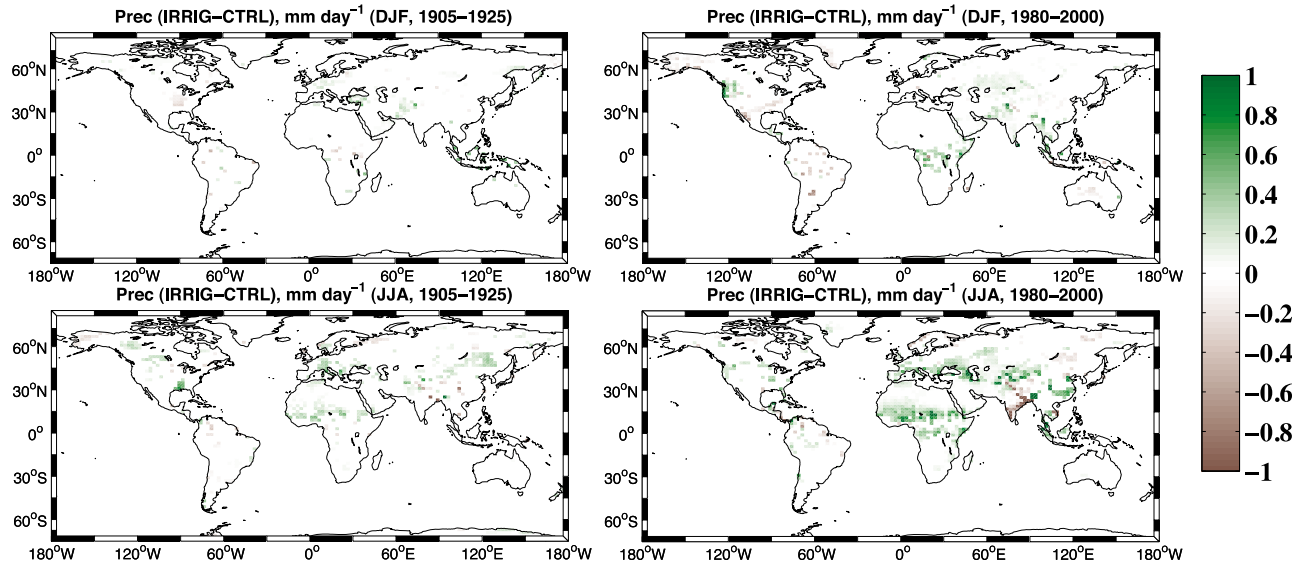

Figure 6. Change in seasonal precipitation (mm/day) induced by irrigation (IRRIG minus CTRL run) for DJF and JJA. (left) Mean for early 20th century (1905–1925). (right) Mean for late 20th century (1980–2000). Only changes that are over land (60°S–90°N) and have a significance level of $p < 0.1$ (based on a two sample t test) are presented.

increased humidity comes primarily from increased moisture advection into these regions, driven by low-pressure anomalies over the north Pacific and northern Eurasia. Over North America, the moisture comes from the Pacific ocean; over Eurasia the moisture comes from the Caspian sea.

[23] While the precipitation response to irrigation is, in some cases, a downwind increase from heavily irrigated areas, it is also often an indirect response due to changes in atmospheric circulation. Figure 6 shows that early in the century, there are isolated instances of precipitation change during boreal winter. For example, small (~0.2 mm d^{-1}) DJF precipitation increases occur over Western Asia, while similarly small but significant decreases are found for the central United States. In the latter part of the century, enhanced (>0.2 mm d^{-1}) DJF precipitation is found, especially in Southern and Southeastern Asia, Central Africa, and the Pacific Northwest. Of these regions, the precipitation enhancements found in Central Africa and the Pacific

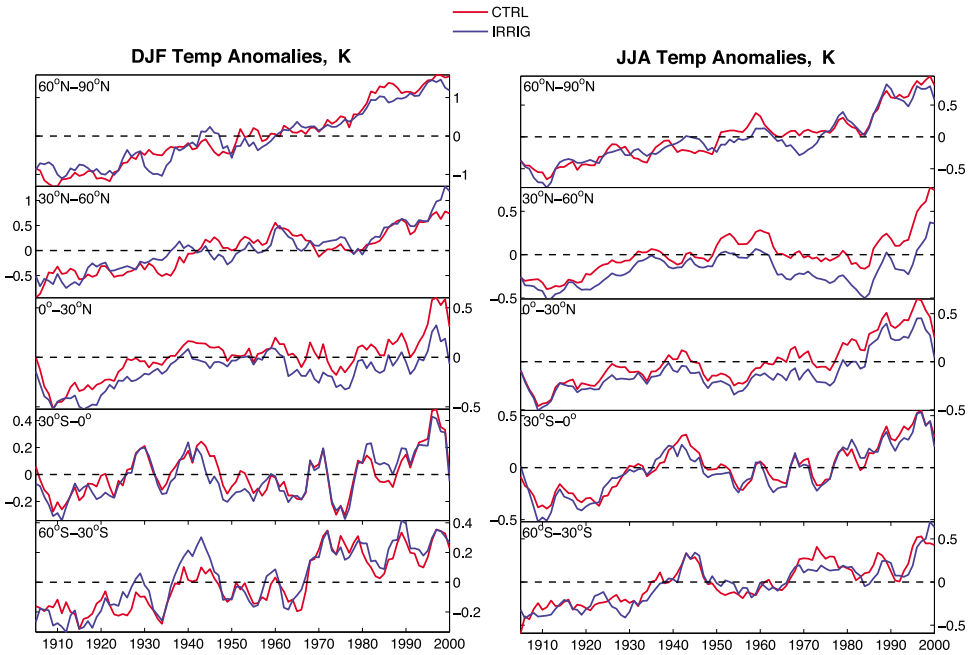

Figure 7. Ensemble mean (2 m) temperature anomalies (K) for DJF and JJA by latitude band relative to the simulated 1905–2000 climate of the CTRL run. Note the scale is not the same for all subplots.

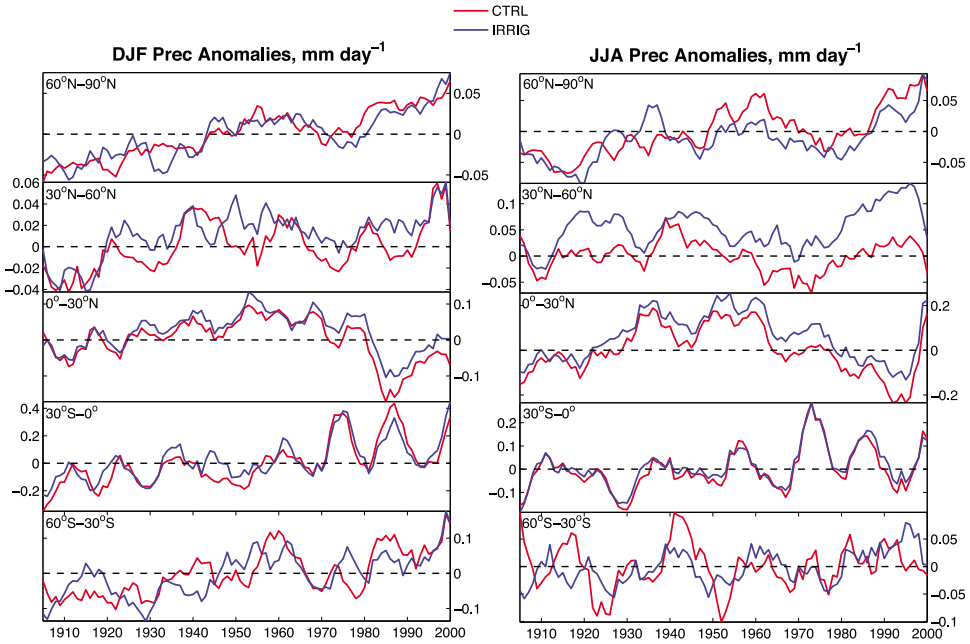

Figure 8. Ensemble mean precipitation anomalies (mm d^{-1}) for DJF and JJA by latitude band relative to the simulated 1905–2000 climate of the CTRL run. Note the scale is not the same for all subplots.

Northwest are clearly due to indirect irrigation effects, because there are no heavily irrigated areas in the vicinity of these regions for DJF. At the same time, decreases in 1980–2000 precipitation for DJF are found in portions of North and South America (0.1 mm d^{-1} to 0.3 mm d^{-1}).

[24] Precipitation responses during boreal summer are more spatially extensive and of greater magnitude than for boreal winter. During JJA of 1905–1925, precipitation increases are found mainly in the central United States, Central Europe, the Sahel, and Eastern Asia. In this case, the Sahel is experiencing precipitation increases because of atmospheric circulation changes. For the 1980–2000 period, more intense precipitation is evident in the Sahel region, the Mediterranean Basin, Southern Europe, and Western, Central, and Eastern Asia. For this period, we see that the dynamical effects of irrigation have intensified for the Sahel and produce more substantial increases in precipitation (0.2 mm d^{-1} to 1.0 mm d^{-1}) there. These precipitation changes appears to be part of a larger-scale shift in the tropical rain belts in our IRRIG simulations. Another striking precipitation change related to monsoon dynamics is found in the south and east portions of the Indian subcontinent, where precipitation is reduced (also 0.2 mm d^{-1} to 1.0 mm d^{-1}).

3.2. Trends and Transient Climate Responses

[25] To look at the time-varying climatic response to irrigation over the 20th century, we spatially average land surface air temperature (Figure 7) and precipitation (Figure 8) over the same latitude bands shown for irrigation in Figure 2. Unsurprisingly, we find the largest cooling for the seasons and latitude bands with the greatest irrigation amounts during the 20th century (i.e., JJA in 30°N–60°N, JJAin 0°–30°N, and DJF in 0°–30°N). For JJA in the 30°N–60°N band, temperatures in the IRRIG run are consistently cooler throughout the century, with the differences increasing after 1950. Cooling in the 0°–30°N band occurs for both JJA and DJF irrigation starting around 1915, and, in general, the cooling is also larger after midcentury. The other latitude

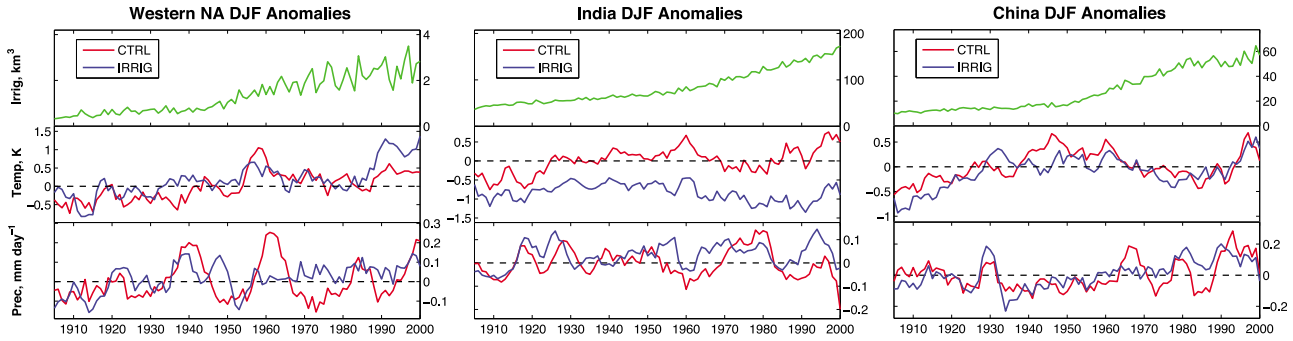

Figure 9. Regional time series of boreal winter (DJF) irrigation, ensemble mean temperature anomalies, and ensemble mean precipitation anomalies for Western North America (130°W–100°W, 30°N–50°N), India (68°E–88°E, 8°N–36°N), and China (98°E–122°E, 22°N–42°N).

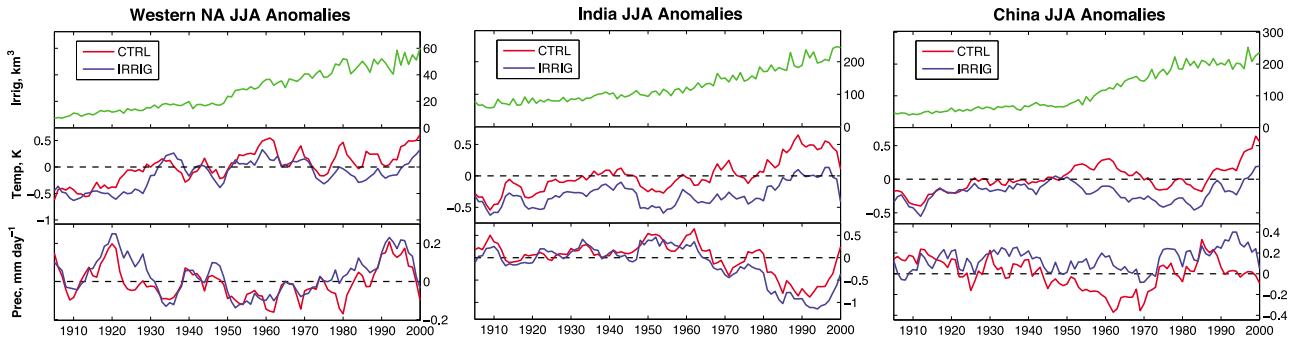

Figure 10. Regional time series of boreal summer (JJA) irrigation, ensemble mean temperature anomalies, and ensemble mean precipitation anomalies for Western North America (130°W–100°W, 30°N–50°N), India (68°E–88°E, 8°N–36°N), and China (98°E–122°E, 22°N–42°N).

bands and seasons, which have smaller irrigation amounts, do not have any consistent temperature differences as a result of irrigation. Precipitation is enhanced in the same seasons and latitude bands that show the largest irrigation-induced cooling in the IRRIG ensemble, which correspond to the latitudes and seasons with the greatest irrigation amounts. Also, the overall patterns of interannual variability are similar for temperature and precipitation in each set of runs.

[26] We next present the transient regional effects of irrigation on climate in Figures 9 and 10, respectively, by focusing on three highly irrigated regions. During boreal winter, we have relatively small amounts of irrigation (~0.5–2 km^3/season) in Western North America but more significant irrigation in India (~40–180 km^3/season) and China (~10–60 km^3/season). Considering the small irrigation amounts in Western North America, the temperature and precipitation changes are then largely attributable to dynamical effects. For example, we clearly see the previously discussed DJF warming for the 1980–2000 period, which begins in the mid-1980s. Dynamical effects have also resulted in precipitation changes including its interannual variability. The irrigation effects on temperature are remarkably different for India and China. In India, we find cooler temperatures throughout the century with larger differences for the second half of the century, while no consistent temperature response is found for China. For the Indian region, we find that precipitation is generally larger after 1950 (except for a period in the early 1970s to early 1980s), whereas IRRIG-CTRL differences fluctuate in sign for China.

[27] All three regions see an increase in irrigation for boreal summer (Figure 10) with comparable amounts in India and China, which lead to cooling in all three regions. The spatially averaged cooling for China is largely attributable to the few grid cells where soil moisture controls evapotranspiration, whereas cooling is more spatially expansive for Western North America and India (despite India's areas of warming). During most of the 20th century, precipitation has increased for Western North America and China. For India, we find an overall decrease in the regionally averaged precipitation as a result of the weaker monsoon.

[28] We also calculated temperature (Figure 11) and precipitation (Figure 12) trends for the first (1905–1950) and second (1950–2000) halves of our ensemble runs for the same latitude bands mentioned previously (Figures 7 and 8). The division at 1950 approximately coincides with the acceleration of irrigation water withdrawals and largest temperature and precipitation differences already discussed. In Figure 11, the 1905–1950 period has positive temperature trends for all latitude bands in both seasons, but differences between the IRRIG and CTRL trends are only found to be statistically significant for 4 of the 10 plots. Two of the statistically significant differences are for DJF. The 60°N–90°N band has a reduced linear trend in temperature for the IRRIG run relative to the CTRL run, while the 60°S–30°S band has a larger temperature trend for the IRRIG run. However, irrigation is zero for this northern latitude band and small (relative to highly irrigated areas) for this southern hemisphere band during this period. These temperature trend changes are not likely due to the effects of local (i.e., within-band) irrigation during the DJF season, but may represent irrigation induced changes through an indirect dynamical model response.

[29] The other two bands with significant differences during 1905–1950 period are for boreal summer. The highest Northern Hemisphere band again has statistically significant trend differences, but now the IRRIG run has a more positive linear trend in JJA temperature. Given that JJA irrigation in the 60°N–90°N band is also very small, the changes to the temperature trends are again most likely a consequence of nonlocal irrigation effects. Unlike this northern latitude band, the 0°–30°N band has a less positive trend in JJA temperature but with more significant irrigation (~100 km^3/season). The increasing irrigation within this band and its associated cooling lead to a decreased warming trend (although nonlocal effects could also play a role).

[30] In the second half of the 20th century, irrigation has a greater effect on temperature trends, where statistical significance is found for differences in 8 of the 10 plots. For the boreal winter temperatures of 1950–2000, irrigation increases the slope of the linear trends for three of the latitude bands (30°N–60°N, 30°S–0°, 60°S–30°S), while it decreases in one band (0°–30°N). The less positive DJF trend in the 0°–30°N is likely connected to the rapid increase in irrigation for this band between 1950 and 2000. Although the other three bands have nontrivial DJF irrigation amounts (particularly the 30°N–60°N band), the positive trend in the irrigation amounts is perhaps not large enough to produce a reduced temperature trend. While the slightly more positive

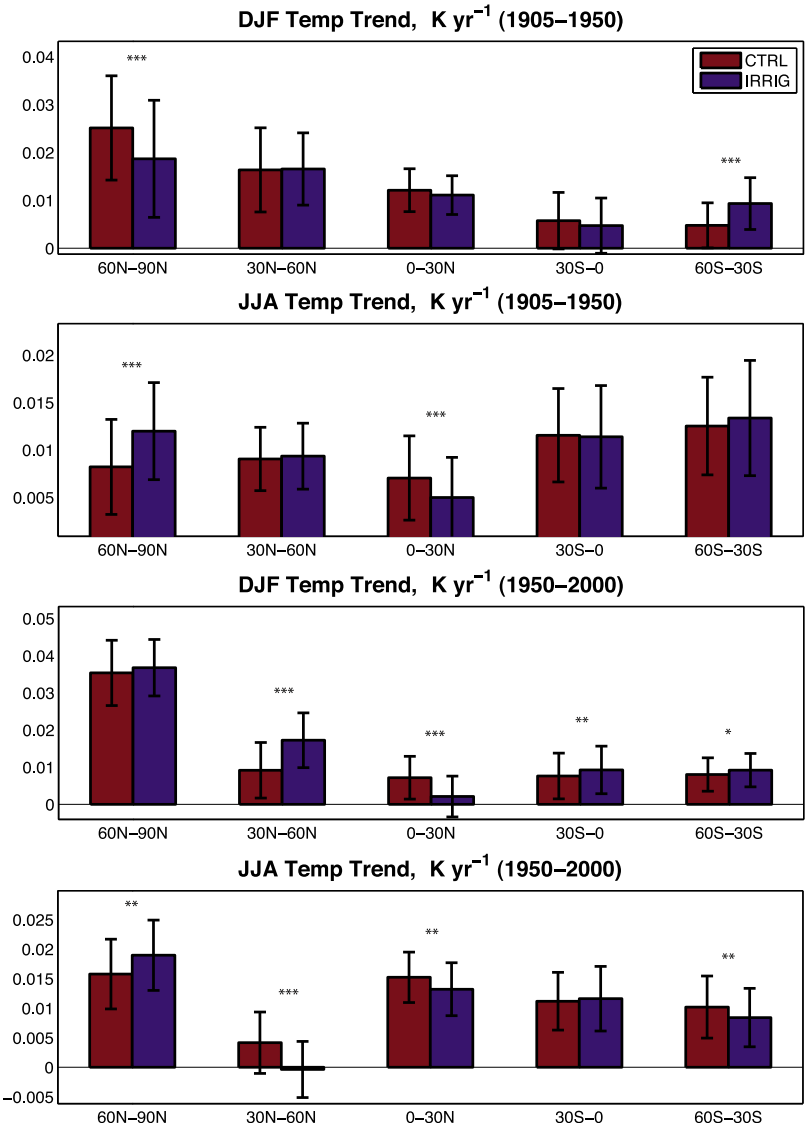

Figure 11. Slope of linear trends in DJF and JJA temperature (K yr^{-1}) for 1905–1950 (top two plots) and 1950–2000 (bottom two plots) by latitude band for the IRRIG and CTRL runs. Single asterisk, double asterisk, and triple asterisk indicate significance at the $p < 0.10$, $p < 0.05$, and $p < 0.01$ levels, respectively, based on a two-sample t test (with the degrees of freedom corrected for serial autocorrelation). Error bars indicate the 95% confidence limits.

trends for the two southern hemisphere bands are not surprising given the uncertainty in predictions, the warming trend for the 30°N–60°N band is unexpected. However, as mentioned earlier, warming in this region is due to increases in the near-surface specific humidity.

[31] The 1950–2000 trends for JJA temperature are reduced in three of the bands, two of which have the most positive trends in irrigation for the period. In fact, the 30°N–60°N band is even slightly negative, which is a reflection of the magnitude and rate at which irrigation increases in this band. As for the JJA trend of 1905–1950, the JJA trend of 1950–2000 is positive for 60°N–90°N.

[32] Figure 12 also shows the linear trend slopes as in Figure 11 but for precipitation rather than temperature. While clear increases in precipitation are apparent in the IRRIG runs relative to the control runs (Figure 8), the links between irrigation and precipitation trends are not as clear. The bands with the most significant irrigation, 30°N–60°N and 0°–30°N, have larger trend slopes in the IRRIG runs compared to the CTRL runs (except for DJF of 1950–2000 in the 30°N–60°N band), but the larger trends are found to be statistically significant in only three cases. The 60°N–90°N band has a less positive trend in the IRRIG run for 1905–1950 and slightly more positive trends for JJA in both halves of the century. Yet, the magnitudes of these differences between the IRRIG and CTRL trends are small in comparison to the magnitudes of the midlatitude trends, which is a reflection of the fact that this band has the lowest irrigation amounts compared to the other latitude bands. The latitude bands with the next two lowest amounts are in the 60°S–30°S and 30°S–0° bands, respectively. Statistically significant differences are found during DJF in the 60°S–

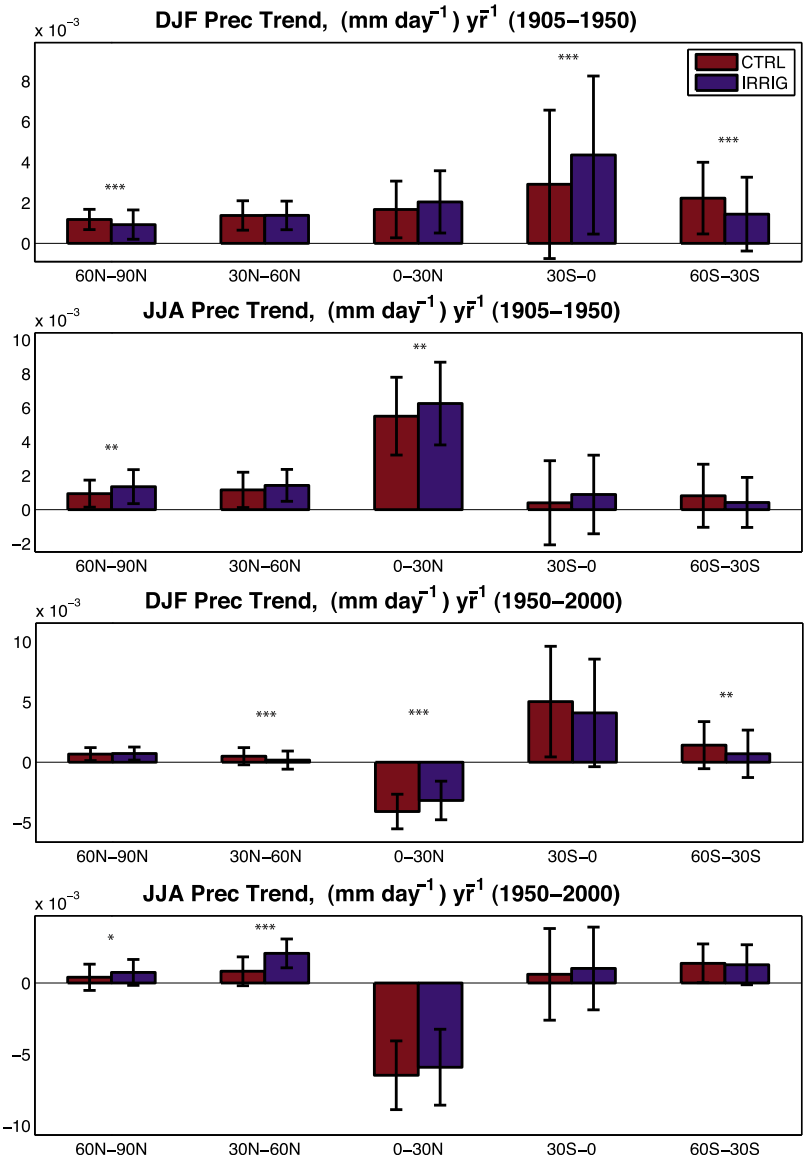

Figure 12. Slope of linear trends in DJF and JJA precipitation ((mm d^{-1}) yr^{-1}) for (top two plots) 1905–1950 and (bottom two plots) 1950–2000 by latitude band for the IRRIG and CTRL runs. Single asterisk, double asterisk, and triple asterisk indicate significance at the $p < 0.10$, $p < 0.05$, and $p < 0.01$ levels, respectively, based on a two-sample t test (with the degrees of freedom corrected for serial autocorrelation). Error bars indicate the 95% confidence limits.

30°S band for both periods, which have a less positive trend. They also occur during DJF 1905–1950 in the 30°S–0° band, which has a more positive trend.

4. Discussion and Conclusions

[33] While there has historically been great interest in understanding the impacts of human-induced land cover changes on the climate system [e.g., *Copeland et al.*, 1996; *Chase et al.*, 2000; *Pielke et al.*, 2002; *Foley et al.*, 2003; *Pitman et al.*, 2004], only recently have available observations and climate models advanced to the level that we can consider the impacts of human management intensity (including irrigation) at the global level [e.g., *Boucher et al.*, 2004; *Lobell et al.*, 2006; *Sacks et al.*, 2009; *Lobell et al.*, 2009]. Here we consider not only the modern-day impacts of observed irrigation on the climate system, but also how these impacts have varied over the course of the 20th century.

[34] Our modern day (1980–2000) irrigation rates are similar in magnitude to two of the three recent studies [*Boucher et al.*, 2004; *Sacks et al.*, 2009] that reported globally averaged temperature and precipitation responses to irrigation (Table 1). *Lobell et al.* [2006], by contrast, kept their irrigated soils essentially saturated, an addition of water that was estimated to be about 100 times modern irrigation amounts [*Sacks et al.*, 2009]. We note, however, that this study was meant to provide an upper bounds to the potential effects of irrigation (but include their estimates in the table because of the dearth of estimates in the literature). Our annual, globally averaged change in temperature from irri-

Table 1. Differences Between Irrigation and Control Runs in Temperature and Precipitation Averaged Over All Land for Recent Studies That Used Global Climate Models[a]

Study	Gross Irrigation (km^3)	ΔTemperature (K)	ΔPrecipitation (mm d^{-1})
Our Study	2565	−0.095	0.026
Sacks et al. [2009]	2560	0.015	0.012
Lobell et al. [2006]	n/a[b]	−1.310	n/a
Boucher et al. [2004]	2353[c]	−0.050	n/a

[a]The values presented for this study are averaged over 1980–2000, for the study of *Sacks et al.* [2009] are for the year 2000, for the study of *Lobell et al.* [2006] are for modern climate, and for the study of *Boucher et al.* [2004] are for the year 1990.

[b]This study was designed to provide an upper bounds on potential irrigation effects rather than to apply realistic irrigation amounts. *Sacks et al.* [2009] performed a sensitivity test to approximate how much water [*Lobell et al.*, 2006] might have added. They report that results similiar to the work of *Lobell et al.* [2006] can be obtained by adding about 100 times more water to the land than is irrigated.

[c]*Boucher et al.* [2004] prescribed the evapotranspiration due to irrigation rather than directly using the gross irrigation reported above; they estimated that the net irrigation corresponding to this value is 1006 km based on the work of *Seckler et al.* [1998].

gation is a cooling over land of about one tenth of a degree; about twice the magnitude of cooling [*Boucher et al.*, 2004] reported and actually of opposite sign compared to the work of *Sacks et al.* [2009], who found an annual average warming (due to a dynamical effect during boreal winter as discussed below).

[35] In Table 2, we compare our seasonal results with the one global irrigation study [*Sacks et al.*, 2009] that reported seasonal changes in temperature and precipitation. Both our study and theirs report cooling with increased precipitation globally in JJA and SON (September, October, and November). The *Sacks et al.* [2009] predictions had reduced magnitude compared to ours (by factor of about 2–3), likely because they only irrigated over the crop fraction of a grid cell instead of the full vegetated fraction of a grid cell, as we did. However, the predictions from the two studies differ more significantly for DJF and MAM (March, April, and May). Our model still predicts cooling and increased precipitation for both of these seasons, but the magnitudes of the changes are smaller. By contrast, *Sacks et al.* [2009] found dramatic warming (accompanied by reduced precipitation) in DJF, which came primarily from dynamical changes: an intensification of the Aleutian low that resulted in warm air advection and significant warming (3 K) over northwest North America. During MAM, *Sacks et al.* [2009] had both warming and increased precipitation, an agreement in sign that did not occur for any other season. We note that our results are an average over the years 1980 to 2000 with transient climate forcings, while those of *Sacks et al.* [2009] were from an equilibrium run for the year 2000.

[36] Generally, we found that irrigation-related climatic impacts increased over the course of the 20th century, especially after about 1950 when irrigation water withdrawals began to accelerate. Temperature impacts (warming and cooling) were mostly colocated with the irrigation regions; affected temperatures trend significantly at least regionally (quite large in some cases), which supports the possibility that irrigation may have masked the global warming signal in certain areas. Precipitation increases occurred primarily down stream from the most highly irrigated areas, except for areas that do not have a corresponding evapotranspiration increase.

[37] Our results also point to the importance of the dynamical effects of irrigation, which are associated with dynamic circulation changes. One of the most striking examples is the increase in precipitation over the Sahel region of Africa, which occurs because of a shift in the tropical rain belts. However, we cannot place a high degree of confidence in these dynamical effects, because they are highly model dependent. Furthermore, these results should be interpreted cautiously, as our model setup is forced with an observed (instead of fully interactive) ocean, which may make evaluation of monsoon dynamics difficult.

[38] Our climatic responses to irrigation, which are governed primarily by changes in the surface Bowen ratio, depend not only on soil moisture increases due to irrigation and precipitation increases, but also on the hydroclimatic regimes that characterize land surface evapotranspiration in the CTRL simulations. *Koster et al.* [2009] describe the two main hydroclimatic regimes as a soil moisture–controlled regime, where changes in soil moisture lead to corresponding changes in evapotranspiration, and an energy-controlled regime, where evapotranspiration is insensitive to soil moisture. As our results demonstrate, despite the significant JJA irrigation in China, we do not see a corresponding increase in evapotranspiration for most of its irrigated areas (Figure 3). The reason is that the majority of these irrigated areas are in a hydroclimatic regime that is energy controlled. Conversely, Western Asia and the Sahel region are soil moisture–limited

Table 2. Differences Between Irrigation and Control Runs in Seasonal Temperature and Precipitation Averaged Over All Land for This Study and Study of *Sacks et al.* [2009][a]

	Our Study	*Sacks et al.* [2009]
	DJF	
Gross irrigation (km^3)	365	266
ΔTemperature (K)	−0.034	0.150
ΔPrecipitation (mm d^{-1})	0.009	−0.008
	MAM	
Gross irrigation (km^3)	526	486
ΔTemperature (K)	−0.069	0.006
ΔPrecipitation (mm d^{-1})	0.006	0.014
	JJA	
Gross irrigation (km^3)	862	871
ΔTemperature (K)	−0.159	−0.056
ΔPrecipitation (mm d^{-1})	0.050	0.027
	SON	
Gross irrigation (km^3)	812	941
ΔTemperature (K)	−0.119	−0.041
ΔPrecipitation (mm d^{-1})	0.038	0.014

[a]The values from this study are averaged over 1980–2000, while the values for *Sacks et al.* [2009] are for the year 2000.

regimes that experience increases to evapotranspiration with additional water (either from irrigation or increased precipitation) infiltrating the soil column.

[39] Besides the actual hydroclimatic regime of an irrigated region, *Lobell et al.* [2009] point out that biases in a climate model's soil moisture are also important for understanding irrigation's impacts. That is, if the goal of irrigation inclusion into a climate model is the improvement of simulated temperatures, then it is necessary to first understand the model's soil moisture biases. For example, *Lobell et al.* [2009] find that irrigation improved simulation of surface air temperature for some regions, but that their model has a known dry bias in soil moisture (likely unrelated to irrigation) and irrigation might simply be compensating for this deficiency. We compared (not shown) our temperature and precipitation anomalies in Figures 7 and 8 to latitude band averages of the Climatic Research Unit (CRU) TS2.1 data sets [*Mitchell and Jones*, 2005]. We find improvements for some periods and latitude bands but less agreement for other times and bands relative to CRU data. However, given our limited understanding of soil moisture biases in the ModelE as well as the uncertainty associated with other transient forcings (e.g., atmospheric composition) and the CRU data itself, it is difficult to conclude anything from such a comparison.

[40] The impact of irrigation in a climate model also depends on how large its effects are relative to those of other climatic forcings [*Lobell et al.*, 2008]. *Sacks et al.* [2009] reviewed studies that compared the climatic impacts of irrigation with those due to land cover change only (excluding other land management effects and only assessing change from potential natural vegetation to current vegetation). At the scale of a climate model's grid cell, they found that these studies [*Matthews et al.*, 2004; *Brovkin et al.*, 1999; *Govindasamy et al.*, 2001; *Zhao et al.*, 2001; *Bounoua et al.*, 2002; *Betts et al.*, 2007] typically report annual cooling effects of up to 0.5–1.0 K with possibly larger seasonal effects, which are almost always less than 2 K. *Sacks et al.* [2009] then contend that land management effects are as important as the effects of land cover change in earth system models. The magnitudes of our regional cooling in Figure 5 also support this contention that irrigation-induced changes in temperature are regionally significant relative to the effects of land cover changes. Further, we find that the significance of the effects has changed over the century. Irrigation had a limited cooling effect over the northwestern portions of the Indian subcontinent and slight cooling (<1 K) elsewhere at the beginning of the 20th century. By century's end, it is transformed into a spatially extensive climate driver, especially in the Northern Hemisphere during both boreal summer (Figure 5).

[41] The results presented herein are likely sensitive to the assumptions of our modeling approach. One of these assumptions, as previously discussed, is the application of irrigation water over the vegetated fractions of the grid cells, which are typically close to 1 for most irrigated areas. To understand how the vegetated and irrigated fractions compare, we compute the grid cell fractions that are equipped for irrigation at a resolution of 2° latitude by 2.5° longitude based on the University of Frankfurt/FAO Global Map of Irrigated Areas [*Siebert et al.*, 2005a]. At this resolution, we find that these irrigated area fractions vary for the major irrigated regions. For the Indian subcontinent, the watershed of the Indus River has irrigated area fractions ranging from approximately 0.4 to 0.8, while the range for Southern India is 0.05 to 0.4. In China, the region around Beijing has values in the 0.2 to 0.5 range, with smaller values (0.05 to 0.2) throughout the rest of the country. The irrigated area fractions are similarly small (~0.05 and 0.25) in Western North America with several grid cells containing ~0.5% irrigated area fractions.

[42] *Sacks et al.* [2009] performed an offline sensitivity test by comparing predictions when irrigation is applied only to the crop fractions (as was done in their coupled simulations) and when it is applied to the entire vegetated fraction (as done here). These authors found that spreading the irrigation out over the vegetated fraction produced a 67% increase in the latent heat flux due to irrigation. It is therefore likely that our modeling approach also overestimates latent heat fluxes. The critical issue is whether irrigating the vegetated fraction modifies soil moisture controls on evapotranspiration as compared to the case where only the actual irrigated areas receive irrigation. For regions with a water-limited evaporative regime in the control run (e.g., Western North America and portions of Southern Asia), evapotranspiration estimates are likely sensitive to the spatial distribution of irrigation within a grid cell. Conversely, in the energy-limited regions of China, the fraction over which irrigation is applied is likely to be less important.

[43] Results are also dependent on our treatment of ocean dynamics. For this study, the use of fixed SST allows for more accurate simulation of climatic trends during the 20th century. However, the results presented herein on the dynamical effects of irrigation suggest that a fully interactive ocean model would be helpful for prediction of atmospheric circulation changes. For example, a more realistic response to temperature contrasts between the land and ocean might lead to better predictions of the climatic changes associated with the Indian monsoon, which has received extensive attention in regional studies [e.g., *Lee et al.*, 2009; *Saeed et al.*, 2009; *Douglas et al.*, 2009].

[44] Irrigation is also important in climate models for efforts to understand sustainability issues and their potential feedbacks on climate. In particular, irrigation is linked to the availability of water resources, which is of great concern in future climate scenarios. For example, *Shen et al.* [2008] and *Alcamo et al.* [2007] investigate potential changes in water availability under various climate change and socioeconomic scenarios using trend estimates and a global hydrology/water use model, respectively. These approaches, which are typical of water resource studies, neglect the coupled feedback between water availability and climate. The coupling between irrigation and climate is an ideal example of these feedbacks, where we generally have cooler temperatures and increased precipitation in the presence of irrigation. If water availability for irrigation decreases in the future, then it is possible that a positive feedback would occur; the resulting reduction in irrigation leading to additional precipitation reduction and warming.

[45] Although irrigation demand is expected to increase in the future, the sustainability of current irrigation rates is uncertain, even without future warming and precipitation changes. One source of this uncertainty is the future availability of groundwater resources [e.g., *Kundzewicz and Döll*, 2009]. Groundwater is a primary source of irrigation water in

the major agricultural regions of the world. *Wisser et al.* [2010] found that current estimates of the groundwater contribution to irrigation for China, India, and the United States are 40%, 50 to 60%, and 65%, respectively. If groundwater sources are not sustainable, then the results of this study and previous studies suggest that it is important to consider climatic impacts alongside food security issues. For example, in India, the region with the largest irrigation-induced cooling, *Douglas et al.* [2009] note that groundwater has been declining by 20 cm/yr for many sections of India [*Bansil*, 2004], with one prediction indicating that groundwater could be depleted regionally by 2025 (S. Jha, Rainwater harvesting in India, available at http://pib.nic.in/feature/feyr2001/fsep2001/f060920011.html, 2001). If Indian irrigation is rapidly reduced after 2025, we might then expect to see additional climatic changes over the subcontinent due to the combined direct and indirect effects of the new irrigation rates.

[46] Future efforts to understand irrigation in a climate model setting should not only carefully document the amount of irrigation water applied to the land, but also keep track of the relative amounts of surface water and groundwater used for irrigation. This irrigation water accounting will promote improved regional predictions of climate for future climate scenarios, especially if widespread depletion of groundwater occurs in the future. Ultimately, other human modifications to the hydrological cycle (e.g., reservoirs) should be incorporated into the next generation of climate models to identify areas that will be subjected to future water availability stress and elucidate the feedbacks between human water use and climate.

[47] **Acknowledgments.** M.J. Puma gratefully acknowledges funding for Interdisciplinary Global Change Research under NASA Cooperative Agreement NNX08AJ75A supported by the NASA Climate and Earth Observing Program. The authors also thank D. Wisser for providing us with the global irrigation data set from *Wisser et al.* [2010] and G. Schmidt for his helpful suggestions. Three anonymous reviewers provided valuable comments that significantly improved this paper (Lamont contribution 7379).

References

Adam, J. C., E. A. Clark, D. P. Lettenmaier, and E. F. Wood (2006), Correction of global precipitation products for orographic effects, *J. Clim.*, *19*, 15–38.

Alcamo, J., M. Flörke, and M. Märker (2007), Future long-term changes in global water resources driven by socioeconomic and climatic changes, *Hydrol. Sci. J.*, *52*(2), 247–275.

Allen, R. G., et al. (1998), Crop evapotranspiration—Guidelines for computing crop water requirements, *FAO Irrig. Drain. Pap. 56, Tech. rep.*, Food and Agric. Organ. of the U. N., Rome.

Ball, J. T., I. E. Woodrow, and J. A. Berry (1987), A model predicting stomatal conductance and its application to the control of photosynthesis under different environmental conditions, in *Progress in Photosynthesis*, edited by I. Biggins, pp. 221–224, Nijhoff, Zoetermeer, Netherlands.

Bansil, P. C. (2004), *Water Management in India*, Concept Publ., New Delhi.

Barnston, A. G., and P. T. Schickedanz (1984), The effect of irrigation on warm season precipitation in the southern Great Plains, *J. Appl. Meteorol.*, *23*(6), 865–888.

Betts, R. A., P. D. Falloon, K. K. Goldewijk, and N. Ramankutty (2007), Biogeophysical effects of land use on climate: Model simulations of radiative forcing and large-scale temperature change, *Agric. For. Meteorol.*, *142*(2–4), 216–233.

Bonfils, C., and D. Lobell (2007), Empirical evidence for a recent slowdown in irrigation-induced cooling, *Proc. Natl. Acad. Sci. U. S. A.*, *104*(34), 13,582–13,587.

Boucher, O., G. Myhre, and A. Myhre (2004), Direct human influence of irrigation on atmospheric water vapour and climate, *Clim. Dyn.*, *22*(6), 597–603.

Bounoua, L., R. DeFries, G. J. Collatz, P. Sellers, and H. Khan (2002), Effects of land cover conversion on surface climate, *Clim. Change*, *52*(1), 29–64.

Brovkin, V., A. Ganopolski, M. Claussen, C. Kubatzki, and V. Petoukhov (1999), Modelling climate response to historical land cover change, *Global Ecol. Biogeogr.*, *8*(6), 509–517.

Chase, T. N., R. A. Pielke, T. G. F. Kittel, R. R. Nemani, and S. W. Running (2000), Simulated impacts of historical land cover changes on global climate in northern winter, *Clim. Dyn.*, *16*(2–3), 93–105.

Copeland, J. H., R. A. Pielke, and T. G. F. Kittel (1996), Potential climatic impacts of vegetation change: A regional modeling study, *J. Geophys. Res.*, *101*(D3), 7409–7418, doi:10.1029/95JD02676.

Diffenbaugh, N. S. (2009), Influence of modern land cover on the climate of the United States, *Clim. Dyn.*, *33*, 945–958.

Douglas, E. M., A. Beltran-Przekurat, D. Niyogi, R. A. Pielke Sr., and C. J. Vörösmarty (2009), The impact of agricultural intensification and irrigation on land-atmosphere interactions and Indian monsoon precipitation—A mesoscale modeling perspective, *Global Planet. Change*, *67*(1–2), 117–128, doi:10.1016/j.gloplacha.2008.12.007.

Farquhar, G. D., S. von Caemmerer, and J. A. Berry (1980), A biochemical model of photosynthetic CO_2 assimilation in leaves of C3 species, *Planta*, *149*, 78–90.

Federer, C. A., C. Vörösmarty, and B. Fekete (2003), Sensitivity of annual evaporation to soil and root properties in two models of contrasting complexity, *J. Hydrometeorol.*, *4*(6), 1276–1290.

Foley, J. A., M. H. Costa, C. Delire, N. Ramankutty, and P. Snyder (2003), Green surprise? How terrestrial ecosystems could affect Earth's climate, *Frontiers Ecol. Environ.*, *1*(1), 38–44.

Freydank, K., and S. Siebert (2008), Towards mapping the extent of irrigation in the last century: Time series of irrigated area per country, *Tech. Rep. Frankfurt Hydrol. Pap. 08*, Inst. of Phys. Geogr., Univ. of Frankfurt, Frankfurt, Germany.

Govindasamy, B., P. B. Duffy, and K. Caldeira (2001), Land use changes and Northern Hemisphere cooling, *Geophys. Res. Lett.*, *28*(2), 291–294, doi:10.1029/2000GL006121.

Haddeland, I., D. P. Lettenmaier, and T. Skaugen (2006), Effects of irrigation on the water and energy balances of the Colorado and Mekong river basins, *J. Hydrol.*, *324*(1–4), 210–223.

Hansen, J., et al. (2007), Climate simulations for 1880–2003 with GISS modelE, *Clim. Dyn.*, *29*(7–8), 661–696.

Koster, R. D., et al. (2004), Regions of strong coupling between soil moisture and precipitation, *Science*, *305*(5687), 1138–1140.

Koster, R. D., S. D. Schubert, and M. J. Suarez (2009), Analyzing the concurrence of meteorological droughts and warm periods, with implications for the determination of evaporative regime, *J. Clim.*, *22*(12), 3331–3341.

Kueppers, L. M., M. A. Snyder, and L. C. Sloan (2007), Irrigation cooling effect: Regional climate forcing by land use change, *Geophys. Res. Lett.*, *34*, L03703, doi:10.1029/2006GL028679.

Kueppers, L. M., et al. (2008), Seasonal temperature responses to land use change in the western United States, *Global Planet. Change*, *60*(3–4), 250–264.

Kundzewicz, Z. W., and P. Döll (2009), Will groundwater ease freshwater stress under climate change?, *Hydrol. Sci. J.*, *54*(4), 665–675.

Lee, E., T. N. Chase, B. Rajagopalan, R. G. Barry, T. W. Biggs, and P. J. Lawrence (2009), Effects of irrigation and vegetation activity on early Indian summer monsoon variability, *Int. J. Climatol.*, *29*(4), 573–581.

Lobell, D. B., G. Bala, and P. B. Duffy (2006), Biogeophysical impacts of cropland management changes on climate, *Geophys. Res. Lett.*, *33*, L06708, doi:10.1029/2005GL025492.

Lobell, D. B., C. Bonfils, and J. M. Faurès (2008), The role of irrigation expansion in past and future temperature trends, *Earth Interact.*, *12*, 1–11.

Lobell, D., G. Bala, A. Mirin, T. Phillips, R. Maxwell, and D. Rotman (2009), Regional differences in the influence of irrigation on climate, *J. Clim.*, *22*(8), 2248–2255.

Matthews, E. (1983), Global vegetation and land use: New high-resolution data bases for climate studies, *J. Appl. Meteorol.*, *22*(3), 474–487.

Matthews, E. (1984), Prescription of land surface boundary conditions in GISS GCM II: A simple method based on fine-resolution data bases, *NASA Tech. Memo*, *86096*, 20 pp.

Matthews, H. D., A. J. Weaver, K. J. Meissner, N. P. Gillett, and M. Eby (2004), Natural and anthropogenic climate change: Incorporating historical land cover change, vegetation dynamics and the global carbon cycle, *Clim. Dyn.*, *22*(5), 461–479.

Mitchell, T. D., and P. D. Jones (2005), An improved method of constructing a database of monthly climate observations and associated high-resolution grids, *Int. J. Climatol.*, *25*(6), 693–712.

Pielke, R. A., Sr. (2001), Influence of the spatial distribution of vegetation and soils on the prediction of cumulus convective rainfall, *Rev. Geophys.*, *39*(2), 151–177.

Pielke, R. A., G. Marland, R. A. Betts, T. N. Chase, J. L. Eastman, J. O. Niles, D. D. S. Niyogi, and S. W. Running (2002), The influence of land use change and landscape dynamics on the climate system: Relevance to climate change policy beyond the radiative effect of greenhouse gases, *Philos. Trans. R. Soc. London A*, *360*(1797), 1705–1719, doi:10.1098/rsta.2002.1027.

Pitman, A. J., G. T. Narisma, R. A. Pielke, and N. J. Holbrook (2004), Impact of land cover change on the climate of southwest Western Australia, *J. Geophys. Res.*, *109*, D18109, doi:10.1029/2003JD004347.

Ramankutty, N., and J. A. Foley (1999), Estimating historical changes in global land cover: Croplands from 1700 to 1992, *Global Biogeochem. Cycles*, *13*(4), 997–1027.

Rayner, N. A., D. E. Parker, E. B. Horton, C. K. Folland, L. V. Alexander, D. P. Rowell, E. C. Kent, and A. Kaplan (2003), Global analyses of sea surface temperature, sea ice, and night marine air temperature since the late nineteenth century, *J. Geophys. Res.*, *108*(D14), 4407, doi:10.1029/2002JD002670.

Rosenzweig, C., and F. Abramopoulos (1997), Land surface model development for the GISS GCM, *J. Clim.*, *10*, 2040–2054.

Sacks, W. J., B. I. Cook, N. Buenning, S. Levis, and J. H. Helkowski (2009), Effects of global irrigation on the near-surface climate, *Clim. Dyn.*, *33*(2), 159–175.

Saeed, F., S. Hagemann, and D. Jacob (2009), Impact of irrigation on the South Asian summer monsoon, *Geophys. Res. Lett.*, *36*, L20711, doi:10.1029/2009GL040625.

Schmidt, G. A., et al. (2006), Present-day atmospheric simulations using giss modele: Comparison to in situ, satellite, and reanalysis data, *J. Clim.*, *19*(2), 153–192.

Seckler, D., U. Amarasinghe, D. Molden, R. de Silva, and R. Barker (1998), *World Water Demand and Supply, 1990 to 2025: Scenarios and Issues*, Int. Water Manage. Inst., Colombo, Sri Lanka.

Shen, Y., T. Oki, N. Utsumi, S. Kanae, and N. Hanasaki (2008), Projection of future world water resources under SRES scenarios: Water withdrawal, *Hydrol. Sci. J.*, *53*(1), 11–33.

Siebert, S., P. Döll, S. Feick, and J. Hoogeveen (2005a), Global map of irrigated areas version 2.2, *Tech. Rep.*, Johann Wolfgang Goethe Univ., Frankfurt, Germany.

Siebert, S., P. Döll, J. Hoogeveen, J. M. Faures, K. Frenken, and S. Feick (2005b), Development and validation of the global map of irrigation areas, *Hydrol. Earth Syst. Sci.*, *9*(5), 535–547.

Tian, X., A. Dai, D. Yang, and Z. Xie (2007), Effects of precipitation-bias corrections on surface hydrology over northern latitudes, *J. Geophys. Res.*, *112*, D14101, doi:10.1029/2007JD008420.

Vörösmarty, C. J., B Moore, A. L. Grace, M. P. Gildea, J. M. Melillo, B. J. Peterson, E. B. Rastetter, and P. A. Steudler (1989), Continental scale models of water balance and fluvial transport: An application to South America, *Global Biogeochem. Cycles*, *3*(3), 241–265.

Vörösmarty, C. J., C. A. Federer, and A. L. Schloss (1998), Potential evaporation functions compared on us watersheds: Implications for global scale water balance and terrestrial ecosystem modeling, *J. Hydrol.*, *207*, 147–169.

Vörösmarty, C. J., P. Green, J. Salisbury, and R. B. Lammers (2000), Global water resources: Vulnerability from climate change and population growth, *Science*, *289*(5477), 284–288.

Wisser, D., S. Frolking, E. M. Douglas, B. M. Fekete, C. J. Vörösmarty, and A. H. Schumann (2008), Global irrigation water demand: Variability and uncertainties arising from agricultural and climate data sets, *Geophys. Res. Lett.*, *35*, L24408, doi:10.1029/2008GL035296.

Wisser, D., B. M. Fekete, C. J. Vörösmarty, and A. H. Schumann (2010), Reconstructing 20th century global hydrography: A contribution to the Global Terrestrial Network-Hydrology (GTN-H), *Hydrol. Earth Syst. Sci.*, *14*, 1–24.

Zhao, M., A. J. Pitman, and T. N. Chase (2001), The impact of land cover change on the atmospheric circulation, *Clim. Dyn.*, *17*(5), 467–477.

B. I. Cook and M. J. Puma, NASA Goddard Institute for Space Studies, 2880 Broadway, New York, NY 10025, USA. (bc9z@ldeo.columbia.edu; mpuma@giss.nasa.gov)